Article
Chinese Science Bulletin
Progress of Projects Supported by NSFC
SPECIAL TOPIC: Multifunctional Nanocarriers for Biomedical Applications
November 2012 Vol.57 No.31: 3994–4004
doi: 10.1007/s11434-012-5307-8

Novel PLGGE graft polymeric micelles for doxorubicin delivery

YU ZuXiao[1,2], HE Bin[1], SHENG MingMing[1], WANG Gang[1] & GU ZhongWei[1*]

[1] *National Engineering Research Center for Biomaterials, Sichuan University, Chengdu 610064, China;*
[2] *College of Material and Chemical Engineering, Sichuan University of Science & Engineering, Zigong 643000, China*

Received January 15, 2012; accepted April 11, 2012; published online July 10, 2012

Novel poly{(lactic acid)-*co*-[(glycolic acid)-*alt*-(L-glutamic acid)]}-g-monomethyl poly(ethylene glycol) (PLGGE) micelles were prepared and used as carriers for anti-tumor drug delivery. Three PEGylated PLGG copolymers (PLGGE2000, PLGGE1100 and PLGGE500) were characterized by XRD, TG and DSC. The critical micelle concentrations (CMCs) of the amphiphilic copolymers were 1.04, 0.55 and 0.13 μg/mL, respectively. The TEM, AFM and DLS measurements revealed that the micelles were homogeneous spherical nanoparticles with the diameters ranged from 50 to 150 nm when THF was used as solvent in the preparation of the micelles. Interestingly, extended cylindrical micelles were obtained using $CHCl_3$ as solvent. The micelles could trap doxorubicin (DOX) in the core with the highest drug loading content up to 23.7%. The mean diameter of drug loaded micelles was much bigger than that of blank micelles. The *in vitro* drug release of the micelles was diffusion-controlled release within the first 36 h and initial burst release was not obvious. However, after 36 h, the release rate in pH 5.0 was faster than that in pH 7.4 due to the degradation. The PLGGE micelles were nontoxic to both NIH 3T3 fibroblasts and HepG2 cells. The *in vitro* cytotoxicity against HepG2 cells demonstrated that the drug loaded micelles exhibited high inhibition activity to cancer cells. CLSM observation of HepG2 cells showed that DOX released from the micelles could be delivered into cell cytoplasm and cell nuclei. PLGGE micelles are potential promising carriers for anti-tumor drug delivery.

PLGGE, micelles, drug delivery, doxorubicin

Citation: Yu Z X, He B, Sheng M M, et al. Novel PLGGE graft polymeric micelles for doxorubicin delivery. Chin Sci Bull, 2012, 57: 3994–4004, doi: 10.1007/s11434-012-5307-8

Doxorubicin (DOX) is a promising broad-spectrum anticancer drug with high potency against many types of solid cancers including breast cancer, lung cancer, liver cancer, etc. [1,2], and it has achieved remarkable success in early clinical trials [3]. Despite DOX's potency, its application was largely hampered because of its poor water-solubility [4], stability, drug resistance and a number of side effects to normal tissues [5,6]. One way to resolve these problems is to encapsulate the drug into biodegradable polymer micelles. As promising antitumor drug carriers, polymer micelles have attracted much attention for the delivery of drug due to their excellent properties such as high solubilization of hydrophobic drugs (avoiding phagocytic and renal clearance) [7], controllable drug release, selectively targeting delivery [8], low toxicity in normal cells and high stability of drugs *in vitro* and *in vivo*. Polymeric micelles with size ranged from 10 to 100 nm could also avoid the clearance of reticuloendothelial system (RES) [9] and passively accumulated in tumor tissue via the enhanced permeability and retention (EPR) effect [10,11].

Long circulation time in bloodstream is the prerequisite for self-assembly micelles as drug carriers. Poly(ethylene glycol)(PEG) is a biocompatible, non-toxic and water-soluble biomaterial. Micelles containing PEG grafts or blocks would form a hydrated shell on the surface of micelles. It could effectively inhibit protein adsorption, secondary aggregation and reticuloendothelial system uptake, thus leading to higher stability and longer circulation times [12], its uptake by cells [13], and prolonged plasma half-lives [14]. Hydrophobic segments of micelles were critical in drug loading content and efficiency and release rate [15]. Poly (L-lactic acid) (PLLA) was widely studied as hydro-

*Corresponding author (email: zwgu@scu.edu.cn)

phobic segments for its good biodegradability and low immunogenicity [16,17]. However, the application of the PLA is limited due to the high crystallinity, and the acidic degradation product of PLA would cause acute inflammation. Morpholine-2,5-dione derivative and its copolymers were good drug carriers with biocompatibility, biodegradability, non-acid degradation products and no crystallinity [18–20]. Copolymers of L-lactide and morpholine-2,5-dione derivative combined the properties of both PLLA and poly [morpholine-2,5-dione] [19,21]. As hydrophobic segments in micelles, they would not only alleviate the inflammation response and high crystallinity, but also improve the drug release performance. The synthesis of poly{(lactic acid)-*co*-[(glycolic acid)-*alt*-(L-glutamic acid)]} (PLGG) was firstly reported by Deng et al. [21]. Guan et al. [22–24] synthesized PLGG-*b*-PEG-*b*-PLGG, PLGG(-paclitaxel)-*b*-PEG-*b*-PLGG (-paclitaxel) and PLGG(-glucose)-*b*-PEG-*b*-PLGG(-glucose) triblock copolymers, which self-assembled micelles. To our knowledge, there were rare reports on micelles composed of graft copolymer poly{(lactic acid)-*co*-[(glycolic acid)-*alt*-(L-glutamic acid)]}-g-monomethyl poly(ethylene glycol) (PLGGE) for DOX delivery.

In this paper, we synthesized a series of graft copolymer poly{(lactic acid)-*co*-[(glycolic acid)-*alt*-(L-glutamic acid)]}-g-monomethyl poly(ethylene glycol) (PLGGE). The properties of PLGGE copolymers were characterized by XRD, TG and DSC. The PLGGE polymers self-assembled micelles with PLGG as core and mPEG as shell. Anti-tumor drug doxorubicin was encapsulated in the micelles (Scheme 1). The properties of PLGGE micelles including critical micelle concentration (CMC), morphology and size were explored. Especially, the morphology of PLGGE micelles prepared using different organic solvent was investigated by AFM. The *in vitro* release profiles of drug loaded micelles were investigated in two different buffered solutions (pH 7.4 and 5.0). The NIH 3T3 fibroblasts and liver cancer cells HepG2 were incubated with blank micelles to evaluate the cytotoxicity. The drug loaded micelles were incubated with HepG2 cells to evaluate the *in vitro* anticancer effects.

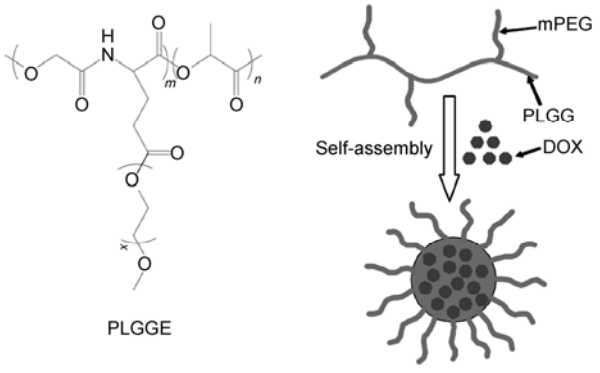

Scheme 1 The schematic self assembly of drug loaded PLGGE micelles.

1 Materials and methods

1.1 Materials

γ-benzyl L-glutamate (BLG), L-Lactide (LLA), stannous octanoate ($SnOct_2$), pyrene (>99%), palladium on activated charcoal (Pd/C, 10%), dicyclohexylcarbodiimide (DCC), dimethylaminopyridine (DMAP), and monomethyl poly (ethylene glycol) of M_W=2000, 1100 and 500 (mPEG) were purchased from Sigmae Aldrich. Doxorubicin hydrochloride (>99%, Sigmae Aldrich) was deprotonated by dissolving in water (2 mg/mL) and adjusted to pH 9.6 to obtain the hydrophobic DOX [25]. Dulbecco's modified Eagle's medium (DMEM), 100× mycillin, and fetal bovine serum were used for cytotoxicity test. Dichloromethane, chloroform, toluene and dimethyl sulfoxide (DMSO) were dried by refluxing over CaH_2 and distilled before use. All other solvents (obtained from Kelong Chemical Co. Chengdu, China) were ACS grade and used as-received.

1.2 Synthesis and characterizations of the PLGGE graft copolymer

The synthesis of (3s)-3-benzoxylcarbonylethyl-morpholine-2,5-dione (BEMD) was performed by the reaction steps as described in the literature [19]. The poly[LA-*co*-(Glc-*alt*-Glu(Bz)), 92:8] (PLGBG) was synthesized by ring-opening copolymerization of both BEMD (100 mg, 0.361 mmol) and LLA (598 mg, 4.151 mmol) using $SnOct_2$ as catalyst, i.e. 8% mole content of BEMD in feed. The PLGBG (92:8) was deprotected by the catalytic (Pd/C) hydrogenation reaction to yield poly[LA-*co*-(Glc-*alt*-Glu)] (PLGG, 5K) containing pendant carboxyl groups. A series of mPEG2000, mPEG1100 and mPEG500 were respectively linked to the pendant carboxyl groups of PLGG (92:8, 5K) in the presence of DCC and DMAP to yield the PLGG (92:8, 5K)-g-mPEG (PLGGE). ^{1}H NMR (a Bruker AV-400 MHz, $CDCl_3$, δ, ppm): 2.19–2.76 (C**H**$_2$C**H**$_2$COO), 4.61 (NHC**H**), 4.84 (COC**H**$_2$), 6.05(N**H**), 5.16 (C**H** of lactic acid), 1.58 (C**H**$_3$ of lactic acid), 3.38 (—OC**H**$_3$ of the pendant mPEG), 3.65 (—OC**H**$_2$C**H**$_2$— of the pendant mPEG).

The TGA of the mPEG, PLGG and PLGGE samples was performed on a NETZSCH instrument (Germany). Approximate 3–4 mg of sample was heated from 35 to 600°C at a heating rate of 10°C/min under a nitrogen purge of 30 mL/min.

The differential scanning calorimetric (DSC) experiments were performed on a TA System Q100 under nitrogen at a flow rate of 50 mL/min. The samples of PLGG and PLGGE copolymers were heated from −90 to 170°C at a heating rate of 10°C/min.

X-ray diffractometry (XRD) measurements were carried out on a Rigaku D/max-2500 X-ray diffractometer with a CuKα source (γ = 1.78897 nm; 50 kV; 100 mA) in the 2θ range of 7°–40° at a scanning speed of 2.0°/min.

1.3 Preparation and characterization of micelles

For preparation of PLGGE micelles, the copolymer was dissolved in chloroform or THF, and then dropped into the deionized water in a beaker under stirring. The beaker was opened to air with agitation for 24 h. The residual chloroform or THF was removed by rotation evaporator.

Pyrene was used as a fluorescence probe to measure the critical micelle concentration (CMC) of PLGGE. The PLGGE solutions with concentration from 1×10^{-8} to 1.0 mg/mL were shook with pyrene (6.0×10^{-7} mol/L) at 37°C overnight. The fluorescence spectra of each sample under excitation at λ_{em}=395 nm with a scan rate of 240 nm/min were obtained using a Hitachi F-7000 Spectrofluorometer (Japan) at 25°C. The CMC was estimated by plotting the pyrene fluorescence intensity ratio I_{338}/I_{334} against the logarithm of the micelle concentration.

The particle size, size distribution, and morphology of micelles were characterized by dynamic light scattering (DLS, Malvern Zetasizer Nano ZS) instrument, atomic force microscopy (AFM, ECLIPSE Ti-U MFP-3D-BIO) and transmission electron microscopy (TEM, JEM-100CX (JEOL)), respectively.

1.4 Preparation of drug loaded micelles

The DOX loaded micelles were prepared as following [26]: DOX was dissolved in THF (1.1 mg/mL) containing DMSO (3 drops) and stirred for 10 min, and subsequently dropped to 10 mg/mL of PLGGE under stirring. The mixture was opened to air under stirring overnight. After filtration through a syringe filter (pore size: 450 nm) to remove the DOX aggregates, the unincorporated DOX was eliminated by ultrafiltration using regenerated cellulose centrifuge filters (MWCO 3.5 kD, USA) through centrifugation (3800 r/min). The product was freeze-dried. The amount of entrapped DOX was measured by UV absorbance at 485 nm (UV-Vis, Lambda 650). The drug loading content (DLC, %) and encapsulation efficiency (EE, %) were calculated by the following equation:

$$\text{DLC} = (\text{weight of DOX in micelles})/(\text{weight of drug loaded micelles})\times100\%, \quad (1)$$

$$\text{EE} = (\text{weight of DOX in micelles})/(\text{weight of DOX in feed})\times100\%. \quad (2)$$

1.5 *In vitro* DOX release profile

The *in vitro* release of DOX from PLGGE micelles suspension (1.0 mL, DLC 10 wt%) in MWCO 3500 Da dialysis bags was determined in a vial containing 25 mL of phosphate buffered saline (PBS, 0.01 mol/L) with pH 7.4 and 5.0. The vials were put in a shaking bed with the shaking rate of 120 r/min at 37°C. At scheduled time intervals, 5 mL of the dialysis buffer was taken out and replaced with another equal volume of fresh PBS. The measurement of the DOX concentration in the dialysate was performed by measuring the absorbance at 485 nm with a UV-Visible spectrophotometer (Lambda 650). The release was carried out in triplicate and the average was showed. As control, the release profile of free DOX was tested using the same method.

1.6 Cell culture

Liver cancer cell HepG2 and NIH 3T3 fibroblasts were respectively cultured in Dulbecco's Modified Eagle's Medium (DMEM) supplemented with 10% fetal bovine serum (Chengdu Halibio Co., Ltd., China), 100 IU/mL penicillin and 100 μg/mL streptomycin at 37°C in a humidified atmosphere of 5% CO_2. Subsequently, HepG2 and 3T3 cells were respectively plated at a cell density of 5×10^3 cells per well in a 96-well plate in 100 μL of medium and incubated for another 24 h. The resulted cell suspension was used in the following experiments.

1.7 Safety of micelles

The cytotoxicity of blank micelles was evaluated by co-culturing the micelles with HepG2 and NIH 3T3. The two cell lines were cultured for 24 h in 96-well plates (5×10^3 cells per well) in Dulbecco's Modified Eagle's Medium (DMEM) supplemented with 10% fetal bovine serum, 100 IU/mL penicillin and 100 μg/mL streptomycin. The culture media were replaced by media containing different concentrations of PLGGE2000 micelles. After 48 h incubation, the cell viability was evaluated by MTT assay.

1.8 Cytotoxicity of micelles

HepG2 cells were seeded onto 96-well plates at 5×10^3 cells per well and incubated for 24 h (37°C, 5% CO_2). Then the culture medium was replaced with 100 μL of the fresh culture medium containing free DOX or DOX loaded micelles at different concentrations. The cells were further incubated for 12, 24, 48 and 72 h. Then, 10 μL of MTT solution (5 mg/mL, in PBS, pH 7.4) was added to each well. After incubated for 4 h, the solution containing unreacted MTT was carefully removed from each well. The blue formazan crystals formed were dissolved with 100 μL of DMSO. The absorbance at 492 nm was measured using a Thermo scientific MK3. The cell viability was calculated by the following formula [27]: Cell viability % = $(I_{sample}/I_{control})\times100\%$, where I_{sample} and $I_{control}$ represent the fluorescence intensity determined for cells treated with different micelles and for control cells (nontreated), respectively.

1.9 Confocal laser scanning microscopy (CLSM)

CLSM was used to examine the intracellular distribution of DOX. HepG2 cells were cultured at 5×10^3 cells per well on 35 mm diameter glass dishes for 24 h. The culture medium

was replaced with fresh medium containing free DOX or drug loaded micelles. After being incubated for 3 and 24 h, the cells were washed three times with PBS (pH 7.4) to remove DOX or DOX loaded micelles outside the cells. Fluorescence intensity was measured by CLSM (Leica TCP SP5) with excitation at 485 nm and emission at 595 nm for DOX.

2 Results and discussion

2.1 Properties of the PLGGE copolymers

The amphiphilic PLGGE graft copolymers with different mPEG side chain lengths were successfully synthesized. The Molecular weight of mPEG were 2000, 1100 and 500, respectively. Thus, the PLGGE2000, PLGGE1100 and PLGGE500 were selected for the following studies.

The X-ray diffraction (XRD) analysis of the three PLGGE polymers is illustrated in Figure 1. The spectrum of PLGGE2000 showed two strongest diffraction peaks at 2θ =19.2° and 23.2° which were the typical crystal of mPEG [28]. The PLGGE2000 also presented relative lower diffraction peaks at 2θ =16.8°. As for PLGGE500, two strongest diffraction peaks appeared at 2θ=16.8° and 19.2°, mainly due to the semi-crystallization of PLGG polymer backbone. Interestingly, the crystal structure of the PLGGE1100 was different from that of the PLGGE2000 and PLGGE500, and only a stronger and rather broader diffraction peak in about 2θ =10°–25° region was observed (Figure 1(b)). It indicated that the conjugation of mPEG with PLGG suppressed the crystallization of both PLGG and mPEG.

The thermal stability of the PLGGE was evaluated using TGA. Thermogravimetric analysis (Figure 2) revealed that the onset of thermal degradation for each sample occurred above 200°C. As references, the PLGG showed a fast

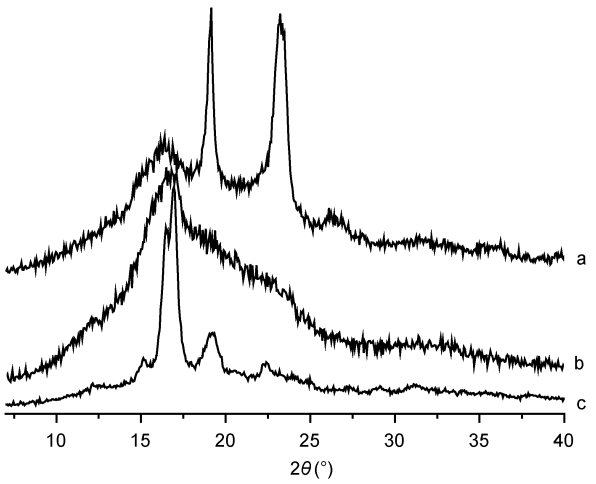

Figure 1 XRD spectra of PLGGE2000 (a), PLGGE1100 (b) and PLGGE500 (c).

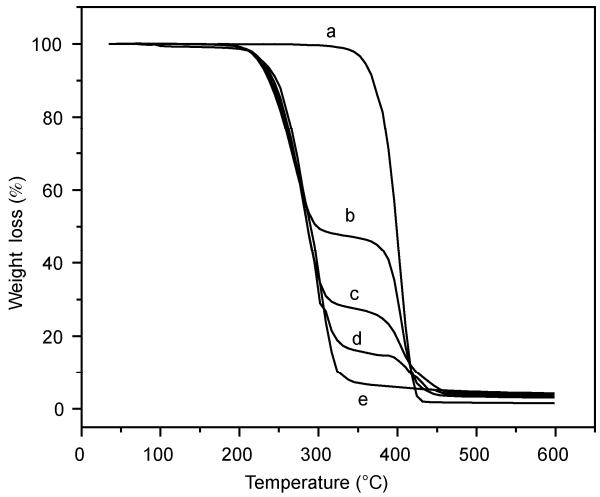

Figure 2 TGA curves of mPEG2000 (a), PLGGE2000 (b), PLGGE1100 (c), PLGGE500 (d) and PLGG (e).

weight loss starting from 240.6 to 340°C while that of mPEG2000 from 383.6 to 430°C. For three PLGGE graft copolymers, the thermal degradation appeared to occur in two steps. The tendency was similar. The first weight losses of three PLGGE copolymers starting from about 233°C were assigned to the decomposition of the polymer backbone (PLGG), while the subsequent weight losses at about 387°C were attributed to the decomposition of the grafted mPEG chains [28]. Furthermore, the PLGGE2000, PLGGE1100 and PLGGE500 lost 51.88%, 72.56% and 84.17% of their weights. When the temperature increased from 387°C, the weight loss of PLGGE2000, PLGGE1100 and PLGGE500 decreased from 44.35%, 23.00% to 11.23%. These results were in good agreement with the mass ratio of mPEG in the copolymers. Additionally, at 500°C or higher, all the weight losses were higher than 98%, it indicated the complete decomposition of the copolymers.

The DSC thermograms of PLGGE are presented in Figure 3 and the calorimetric data are summarized in Table 1. PLGG was a semi-crystalline polymer showing a T_g of 51°C and T_m of 141°C (Figure 3(a)), whereas mPEG2000 was highly crystallized, showing a T_m of 56°C (not shown). Almost the same T_g and T_m for PLGGE500, PLGGE1100 and PLGGE 2000 were observed at approximate 23°C and 136°C, respectively. It was mainly attributed to the PLGGE containing the same polymer backbone (PLGG). For the PLGGE2000, another strong melting peak appeared at 52.4°C, and its ΔH_m value increased remarkably, reflecting the high crystallinity. This was caused by the side chain of mPEG2000. Table 1 showed a slight decrease of T_m from 56°C (in mPEG2000) to 52.4°C in PLGGE2000 copolymer, the graft of mPEG disturbed the crystallization process [28,29]. With the increase of mPEG content, the ΔH_c value of the cold crystallization peak of PLGGE copolymers decreased. The ΔH_c value of PLGGE500 at 77.6°C was seven times stronger than that of PGGE1100 at 85.1°C, while the

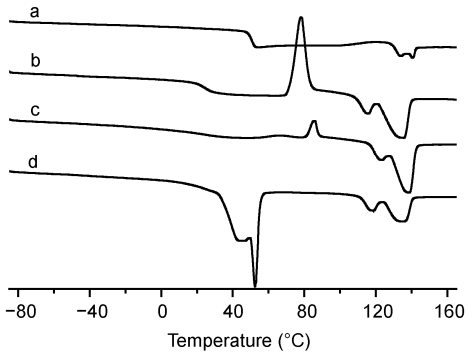

Figure 3 DSC thermograms of PLGG (a), PLGGE500 (b), PLGGE1100 (c) and PLGGE2000 (d).

Table 1 Thermal properties of PLGG, PLGGE500, PLGGE1100 and PLGGE2000

	T_g (°C)	T_m (°C)	ΔH_m (J/g)	T_c (°C)	$-\Delta H_c$ (J/g)
PLGG	51.13	141.10	4.12		
PLGGE500	23.48	134.80	22.03	77.66	19.4
PLGGE1100	22.73	138.17	21.09	85.13	2.73
PLGGE2000	21.65	52.44;135.97	36.12;14.83		

cold crystallization peak of PLGGE2000 was not observed. PLGGE500, PLGGE1100 and PLGGE2000 were semi-crystalline copolymers. The results were strongly supported by XRD study (Figure 1). It has been reported that the semi-crystalline polymers were advantageous compared to the high crystalline polymers when used as a drug delivery carrier due to its high mobility, high permeability and low influence on tissue growth and inflammation [30].

2.2 Characterization of micelles

The three amphiphilic PLGGE copolymers self-assembled the micelles with hydrophobic core and hydrophilic shell. Pyrene was widely used as a fluorescence probe to test the CMCs. As shown in Table 2, the CMC values of PLGGE-2000, PLGGE1100 and PLGGE500 were 1.04×10^{-3}, 0.55×10^{-3} and 0.30×10^{-3} mg/mL, respectively. It was found that the graft copolymers with a larger hydrophobic backbone (PLGG) had a relatively lower CMC. This result implied that the micelles had high stability upon strong dilution in the bloodstream. Furthermore, the decrease in the number of EO units resulted in a small decrease of the CMC, which is consistent with those reported for copolymers [31,32]. The reason was that the decrease of the hydrophilic chain length increased the aggregating tendency of the hydrophobic PLGG segment, which led to a more stable micellar structure with smaller CMC value.

The formation of the self-assembled PLGGE2000, PLGGE1100 and PLGGE500 micelles was further confirmed by AFM measurement as shown in Figure 4 and Table 3. When the micelles were prepared using THF as solvent (Figure 4(a1), (b1) and (c1)), the three micelles clearly showed a homogeneous spherical shape and a narrow size distribution. The mean diameters of the micelles formed by PLGGE2000, PLGGE1100 and PLGGE500 were 50, 90, and 150 nm, respectively. However, when micelles were prepared from $CHCl_3$ as solvent, the cylindrical micelles (Figure 4(b2) and (c2)) were observed apart from a spherical shape of PLGGE2000 micelles (Figure 4(a2)). That meant the formation of cylindrical micelles became easier instead of spherical with the decrease of the hydrophilic mPEG chain length. These results were in agreement with the conclusions that previously reported [33,34]. Such transitions were due to that the increase of the hydrophilic chain length induced greater interfacial curvature [34]. A balance between interfacial tension and chain stretching led to an equilibrium domain morphology and size. Thus, the morphology of PLGGE micelles was controlled via the preparation method and the chain length of mPEG. In addition, the diameters of micelles prepared from $CHCl_3$ were almost consistent with those from THF (Table 3).

Table 2 Properties of blank and DOX loaded PLGGE micelles

Samples	M_n [a] ($\times10^3$)	CMC (μg/mL) [b]	Diameter (nm) [c]		DLC (%)[d]	EE (%)[e]
			Blank micelle	DOX-micelle		
PLGGE2000	10.3	1.04	50	105	12.2	32.3
PLGGE1100	8.7	0.55	78	122	17.9	36
PLGGE500	6.3	0.13	141	220	23.7	40.2

a) Molecular weight obtained from a Waters 510 GPC data (THF as eluent); b) determined using pyrene as a fluorescence probe; c) determined by DLS; d) drug loading content; e) encapsulation efficiency.

Table 3 Physicochemical parameters of PLGGE self-assemble micelles in water

Samples	THF diameter (nm)[a]	Morphology[b]	$CHCl_3$ diameter (nm)[a]	Morphology[b]
PLGGE2000	50	S	50	S
PLGGE1100	90	S	85	C
PLGGE500	150	S	150	C

a) Diameter determined by AFM; b) morphology observed by AFM; S, spherical; C, cylinder.

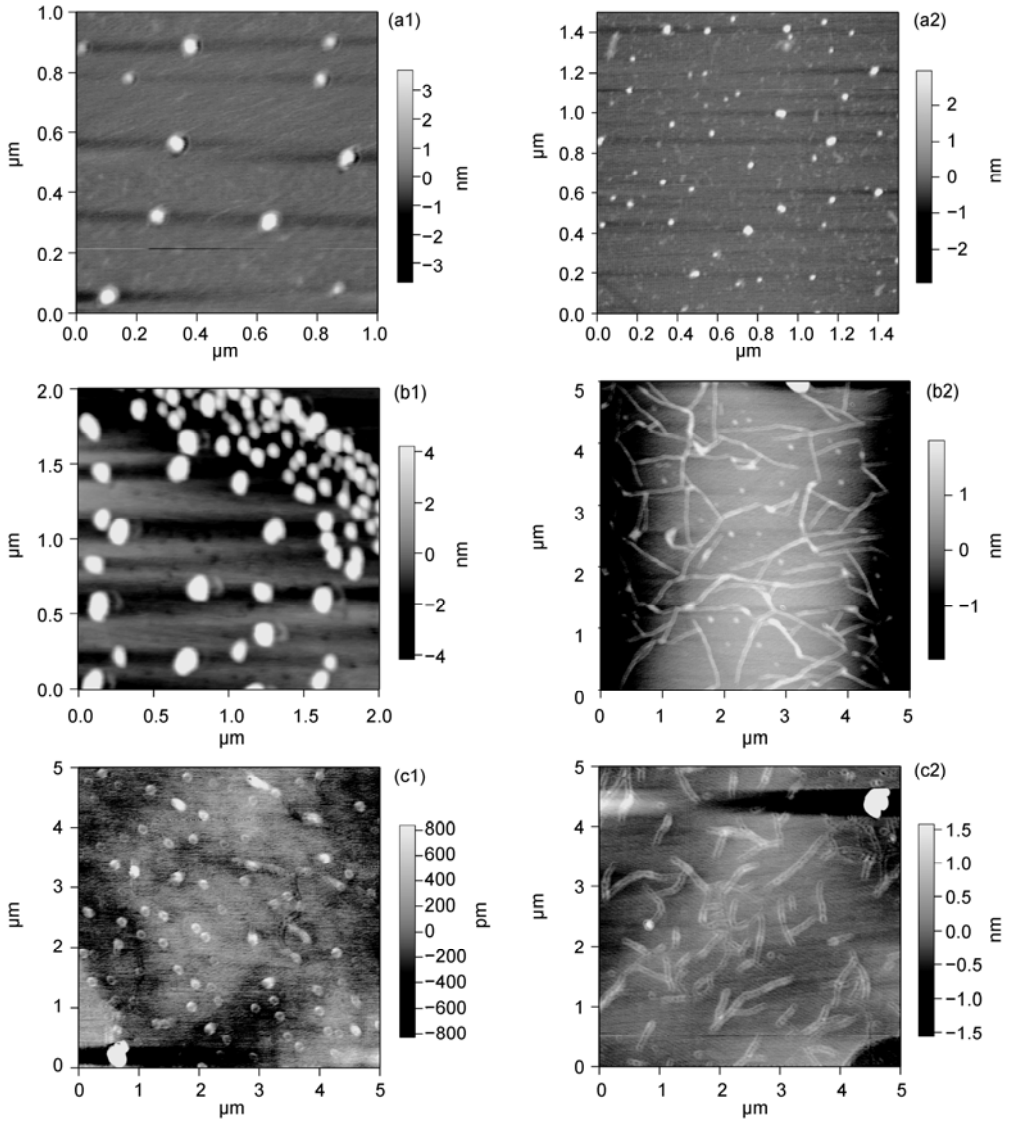

Figure 4 AFM images of PLGGE2000 (a), PLGGE1100 (b) and PLGGE500 (c) micelles. (a1), (b1) and (c1) were prepared using THF as solvent. (a2), (b2) and (c2) were prepared using $CHCl_3$ as solvent. The mean diameters of PLGGE2000, PLGGE1100 and PLGGE500 were 50, 90 and 150 nm, respectively.

2.3 Characterization of empty and DOX loaded micelles

The size distributions and morphology of the empty and DOX loaded PLGGE micelles were determined by DLS and TEM. The mean diameters of the three drug loaded micelles were always larger than those of corresponding empty micelles. DLS (Figure 5) results showed that all self-aggregates had a uniform size distribution. The mean diameter (105 nm) of the drug loaded micelles was 2.1 times larger than that of drug-free micelles (50 nm). It indicated that the enlargement of the particles size was caused by the encapsulated DOX. The increased particle size might be attributed to interactions between DOX and copolymers, further to affect the aggregation of the amphiphic copolymers, thus led to the tremendous differences in average size [35]. TEM (Figure 6) images showed that both the empty and DOX loaded micelles were well dispersed as individual micelles with uniform spherical shape. The results revealed a narrow size distribution with the mean diameters of 38 and 75 nm, respectively. The diameters of spheres observed by TEM were slightly smaller than those by DLS (Figure 5). The reason for this difference was that the mean diameters determined by DLS represented their hydrodynamic diameters after the hydration of mPEG segments, whereas those determined by TEM reflected the dried micelles [36,37].

2.4 Drug loading and *in vitro* drug release

The drug loading content and efficiency of the three micelles are presented in Table 2. The drug loading content and encapsulation efficiency of the micelles were as high as 23.7% and 40.2%. Both drug loading content and encapsulation efficiency increased with decreasing the side chain length of

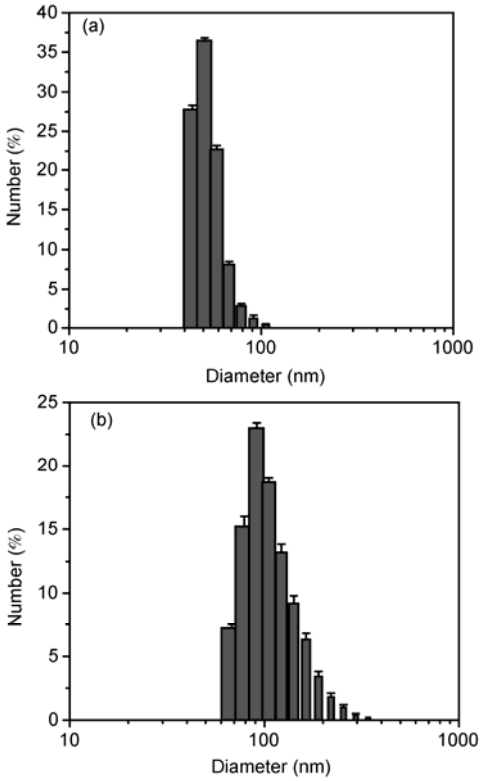

Figure 5 Size distribution of blank (a) and DOX loaded (b) PLGGE2000 micelles determined by DLS. The mean diameters of blank and DOX loaded micelles were 50 and 105 nm, respectively.

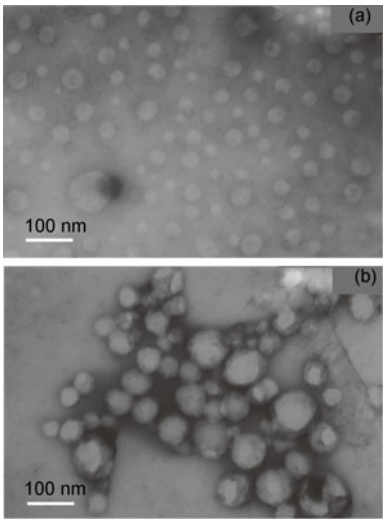

Figure 6 TEM images of blank (a) and DOX loaded (b) PLGGE2000 micelles, the micelles showed unimodal distribution with the mean diameters of 38 and 75 nm, respectively.

mPEG.

The drug release of PLGGE micelles in two different buffered solutions (pH 7.4 and 5.0) are shown in Figure 7. At the same pH value, the accumulated release rate of PLGGE gradually decreased with decreasing the mPEG side chain length. At pH 7.4, the drug release rates of PLGGE 2000, PLGGE 1100 and PLGGE 500 micelles after

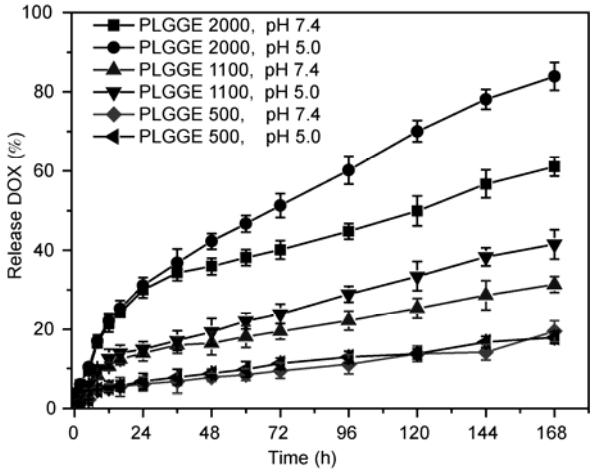

Figure 7 *In vitro* release profiles of DOX from micelle formulations (PLGGE2000, 1100 and 500) at pH 7.4 and 5.0.

168 h were 60%, 31% and 19%, respectively. Because of the shorter hydrophilic side chain length of mPEG, the permeation of water into polymeric cores was more difficult, thus led to the lower diffusion of DOX through the copolymers. Interestingly, at the different pH values (7.4 and 5.0), the effects of pH value on the release of DOX from same polymer micelles were not observed in the first 36 h, mainly due to a slow diffusion-controlled release through the polymer matrix. After 36 h, however, the DOX release from micelles at pH 5.0 was much faster than that at pH 7.4. The faster release of DOX in acidic conditions could be explained as the following reasons: (1) hydrogen bonds were possibly formed between the polymer and DOX at pH 7.4, which could be broken at pH 5.0 [38]; and (2) the degradation of hydrophobic PLGG (micellar core) was faster at pH 5.0 than at pH 7.4 [39]. The degradation rate of the PLGG was also faster than that of PLA. This was mainly attributed to the disruption of the crystallinity caused by the incorporation of L-glutamate residues and the improvement of hydrophilicity due to mPEG segment. For the tumor-targeted DOX delivery, it was important for pH-sensitive releasing behavior to result faster release at acidic conditions in the solid tumor [40]. As decreasing the chain length of mPEG, the effects of pH value on the DOX-release became no more obvious (such as PLGGE500). This could be attributed to the decrease of water solubility of PLGGE. Additionally, no initial burst releases of PLGGE micelles at pH 5.0 and 7.4 were observed, which meant that DOX was largely entrapped in the hydrophobic cores of the micelles.

2.5 Safety of empty micelles

As drug carriers, it is necessary to evaluate the cytotoxicity of the empty micelles using cell viability assay [41]. The cell lines of HepG2 and NIH 3T3 cells were incubated with blank micelles. Figure 8 shows the cell viability of PLGGE-2000 micelles with 48 h incubation. The cell viability of the

micelles with different concentrations in HepG 2 cells was comparable to those of blank control. However, the cell viability of the micelles in NIH 3T3 cells increased with increasing the concentration of the micelles, and it was even higher than 100%. It implied that the high concentration of micelles was in favor of cell proliferation. These results demonstrated that the polymeric micelles were non-toxic.

2.6 Intracellular drug distribution

CLSM was employed to study the cellular uptake and intracellular distribution of DOX loaded micelles in the liver cancer HepG2 cells and the images are shown in Figure 9. After 3 h incubation, the strong red fluorescence of free DOX was observed not only in cell cytoplasm but also nuclei, whereas that of DOX loaded micelles was observed

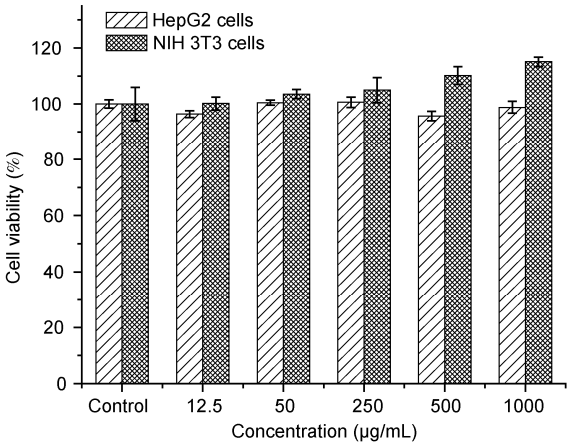

Figure 8 The cytotoxicity of PLGGE2000 blank micelles to HepG2 and 3T3 cells after incubated for 48 h.

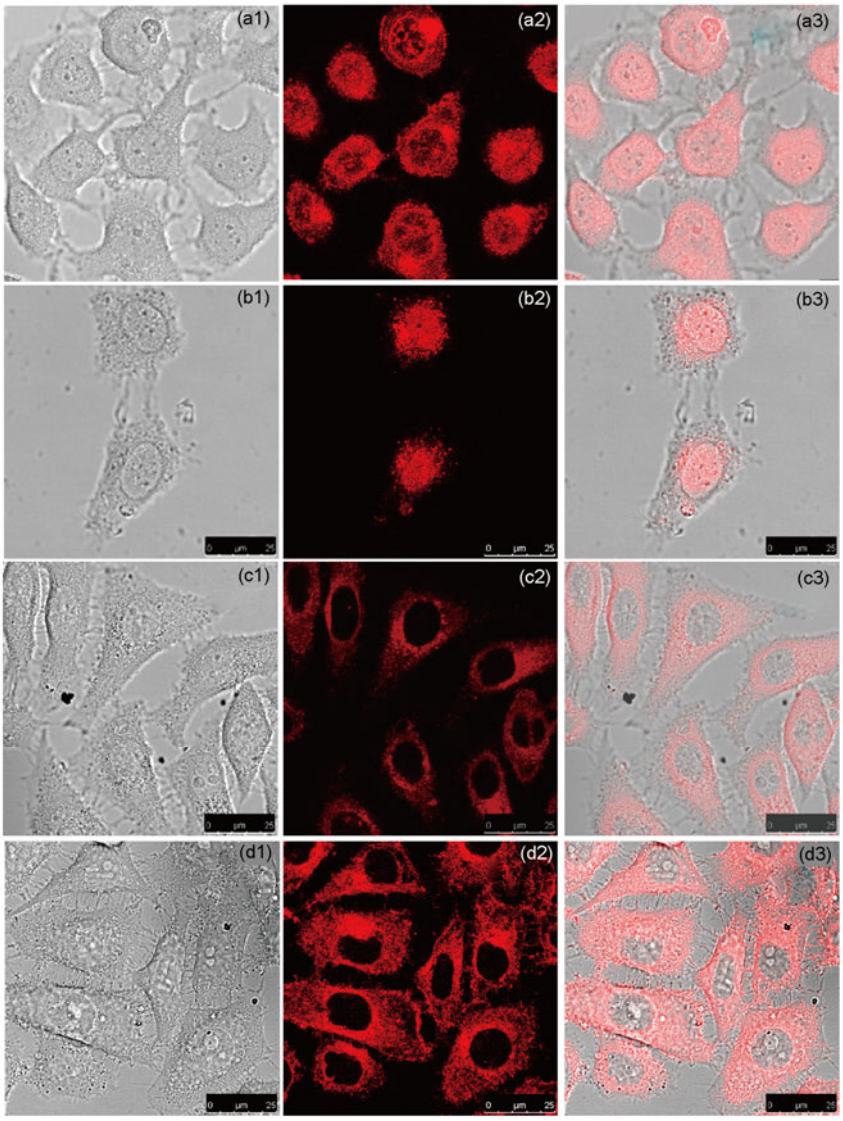

Figure 9 CLSM-images of HepG2 cells after incubated with free DOX for 3 h (a1)–(a3) and 24 h (b1)–(b3), and with DOX loaded PLGGE2000 micelles for 3 h (c1)–(c3) and 24 h (d1)–(d3). (a1)–(d1) The morphologies of cells visualized in the phase-contrast mode; (a2)–(d2) red fluorescence images from excitation of DOX; (a3)–(d3) the overlay of fluorescence channel with bright field.

only in in the cytoplasm rather than the cell nuclei. When the incubation period was elongated to 24 h, the red fluorescence of free DOX was observed only in the nuclei and no red fluorescence was detected in the cytoplasm. However, after DOX loaded micelles were incubated for 24 h, the intensity of red fluorescence obviously increased in cytoplasm. These results showed that the intracellular distribution of the DOX loaded micelles was different from that of free DOX, and it also demonstrated that PLGGE2000 micelle could effectively transport DOX into the cytoplasm, as similarly reported in [25,42]. The internalization mechanism of free DOX was that low molecular weight DOX entered cells via direct permeation through the cellular membrane, while the drug loaded micelles were generally internalized through an endocytosis pathway and localized in endocytic compartments (e.g. endosomes and subsequently lysosomes) [42–45]. For those micelles trapped in endosomes/lysosomes, DOX in PLGGE2000 micelles entered the nuclei much slower than free DOX, as indicated in LCSM measurement. However, DOX in micelles could eventually be delivered into the nuclei to exert its cytotoxicity [46] and inhibit the replication of DNA replication. This was demonstrated by the following cytotoxicity results as shown in Figure 10.

2.7 *In vitro* Cytotoxicity test of the drug loaded micelles

The morphologies of the HepG2 cells after 48 h incubation with the samples are shown in Figure 10. Free and encapsulated DOX could reduce the numbers of tumor cells obviously. Most cells attached and stretched well in empty micelles (Figure 10(b)), almost like control (Figure 10(a)). All the cells exposed to free DOX (10 μg/mL) detached and shrank to spheres (Figure 10(c)). Namely, the free DOX could kill nearly all the tumor cells. For the sample of drug loaded micelles, some cells detached and some stretched well with the same concentration of DOX (Figure 10(d)). This was because the cell endocytosis of the drug loaded micelles into endosomes/lysosomes was influenced by their scaled diameter, and the DOX release from the micelles was relatively slow, thus, both cell morphological changes and alterations in cell numbers confirmed that the anti-tumor effect of drug loaded micelles was inferior to that of free DOX.

The MTT assay was carried out for quantitative analysis in the cytotoxicity of the drug loaded micelles to the HepG2 cells (Figure 11). The quantitative results were coincident to the results in Figure 10. As the drug concentration increased from 0.25 to 20 μg/mL, the cell viabilities of the two samples decreased obviously (Figure 11(a)). When the DOX concentration was 10 μg/mL, free DOX could kill almost all the cells, while only 40% of HepG2 cells were killed by the DOX loaded micelles. In the meanwhile, the IC50 (DOX concentrations that kill 50% of cells) of drug loaded micelles (17.3 μg/mL) was about 6 times higher than that of free drug (3.0 μg/mL) after 48 h incubation. This was due to that free DOX could be readily transported into nuclei by the diffusion mechanism, whereas the micelles were internalized by endocytosis to release the loaded drugs, and the drug diffused through the endocytic compartment membrane to reach the nuclei [44]. Interestingly, to the cell viabilities of free DOX, there was less decrease when the concentration

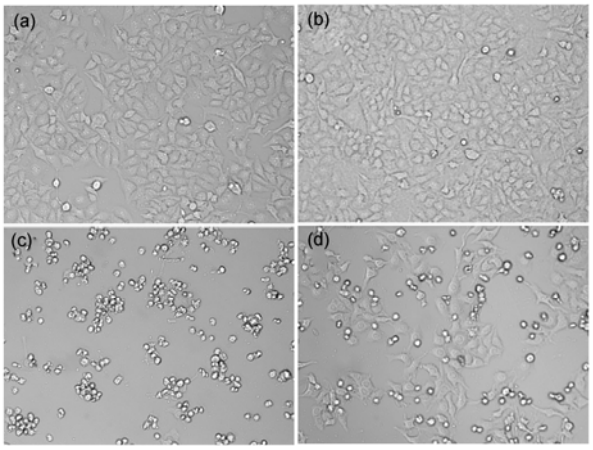

Figure 10 The morphologies of HepG2 cells after 48 h incubation with: (a) cell culture plate as control, (b) blank micelles of PLGGE2000, (c) free DOX and (d) DOX loaded micelles. The concentrations of micelle and DOX were 1000 and 10 μg/mL, respectively.

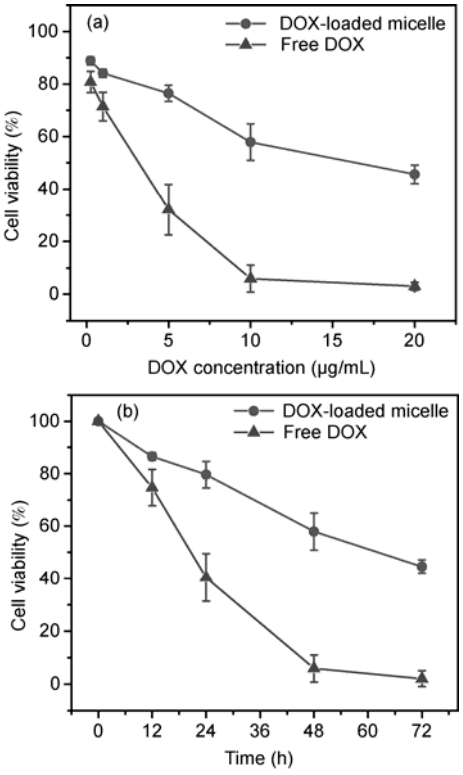

Figure 11 The inhibition effects of HepG2 cells. (a) With various concentrations of the drug after 48 h incubation with DOX loaded micelles and free DOX (the concentration of DOX: 0.25–20 μg/mL); (b) after 12, 24, 48 and 72 h incubation with DOX loaded micelles and free DOX (the concentration of DOX:10 μg/mL).

was more than 10 μg/mL. As shown in Figure 11(b), with the incubation time increasing, the cell viabilities of both free DOX and drug loaded micelles decreased obviously. Hence, higher drug concentration and longer incubation time will cause lower cell viability. It meant the cytotoxicity of the DOX loaded micelles was dependent on the concentration of the drug and incubation time.

3 Conclusions

A series of PLGGE graft copolymers were fabricated. The properties of PLGGE2000, PLGGE1100 and PLGGE500 were characterized by XRD, TG and DSC. The copolymers self-assembled micelles with shell-core structure with the mean diameter ranged from 50 to 150 nm. The CMCs of the micelles varied from 1.04 to 0.13 μg/mL. When the micelles were prepared using THF as solvent, the micelles displayed unimodal size distribution and homogeneous spherical shape. To PLGGE1100 and PLGGE500 copolymers, the extended cylindrical micelles were observed when micelles prepared from $CHCl_3$ as solution. The anti-tumor drug DOX was entrapped in the micelles and the highest drug loading content and efficiency were 23.7% and 40.2%, respectively. The release rate of DOX from the micelles was a slow diffusion-controlled release within the first 36 h and initial burst release was not observed. After 36 h, the release rate in pH 5.0 was faster than that in pH 7.4 due to the degradation-controlled sustained release. The *in vitro* cytotoxicity assay of DOX loaded micelles against HepG2 cells showed that DOX could be efficiently released from the micelles to inhibit the proliferation of cancer cells. CLSM studies showed that the released DOX could be effectively delivered into cells. PLGGE micelles are promising carriers for anti-tumor drug delivery.

This work was supported by the National Basic Research Program of China (*2011CB606206*), *the National Natural Science Foundation of China* (*50830105, 51133004 and 31170921*), *the Key Program for the International S&T Collaboration Projects of China* (*2010DFA51550*), *the Program for New Century Excellent Talents in University, Ministry of Education* (*NCET-10-0564*), *and Department of Education of the Sichuan Province, China* (*09ZC056*).

1 Lee E S, Na K, Bae Y H. Super pH-sensitive multifunctional polymeric micelle. Nano Lett, 2005, 5: 325–329
2 Lai P S, Lou P J, Peng C L, et al. Doxorubicin delivery by polyamidoamine dendrimer conjugation and photochemical internalization for cancer therapy. J Control Release, 2007, 122: 39–46
3 Gabizon A, Shmeeda H, Barenholz Y. Pharmacokinetics of pegylated liposomal doxorubicin: Review of animal and human studies. Clin Pharmacokinet, 2003, 42: 419–436
4 Ganta S, Devalapally H, Shahiwala A, et al. A review of stimuli-responsive nanocarriers for drug and gene delivery. J Control Release, 2008, 126: 187–204
5 Kim J O, Kabanov A V, Bronich T K. Polymer micelles with cross-linked polyanioncore for delivery of a cationic drug doxorubicin. J Control Release, 2009, 138: 197–204
6 Xiong X B, Ma Z, Lai R, et al. The therapeutic response to multifunctional polymeric nano-conjugates in the targeted cellular and subcellular delivery of doxorubicin. Biomaterials, 2009, 31: 757–768
7 Kataoka K, Harada A, Nagasaki Y. Block copolymer micelles for drug delivery: Design, characterization and biological significance. Adv Drug Deliv Rev, 2001, 47: 113–131
8 Lavasanifar A, Samuel J, Kwon G S. Poly (ethylene oxide)-block-poly (lamino acid) micelles for drug delivery. Adv Drug Deliv Rev, 2002, 54: 169–190
9 Liu H, Farrell S, Uhrich K. Drug release characteristics of unimolecular polymeric micelles. J Control Release, 2000, 68: 167–174
10 Maeda H. The enhanced permeability and retention (EPR) effect in tumor vasculature: The key role of tumor-selective macromolecular drug targeting. Adv Enzyme Regul, 2001, 41: 189–207
11 Maeda H, Wu J, Sawa T, et al. Tumorvascular permeability and the EPR effect in macromolecular therapeutics: A review. J Control Release, 2000, 65: 271–284
12 Batrakova E V, Li S, Li Y L, et al. Distribution kinetics of a micelle-forming block copolymer Pluronic P85. J Control Release, 2004, 100: 389–397
13 Keruter J. Nanoparticulate system for brain delivery of drugs. Adv Drug Deliv Rev, 2001, 47: 65–81
14 Bazile D, Prudhomme C, Bassoullet M T, et al. PEG–PLA nanoparticles avoid uptake by the mononuclear phagocytes system. J Pharm Sci, 1995, 84: 493–498
15 Sezgin Z, Yuksel N, Baykara T. Preparation and characterization of polymeric micelles for solubilization of poorly soluble anticancer drugs. Eur J Pharm Biopharm, 2006, 64: 261–268
16 Holland S J, Tighe B J, Gould P L. Polymers for biodegradable medical devices. 1. The potential of polyesters as controlled macromolecular release systems. J Control Release, 1986, 4: 155–180
17 Lee J, Cho E C, Cho K. Incorporation and release behavior of hydrophobic drug in functionalized poly(d,l-lactide)-block-poly(ethylene oxide) micelles. J Control Release, 2004, 94: 323–335
18 Wang D, Feng X D. Synthesis of poly (glycolic acid-*alt*-L-aspartic acid) from a morpholine-2,5-dione derivative. Macromolecules, 1997, 30: 5688–5692
19 Ouchi T, Nozaki T, Okamoto Y, et al. Synthesis and enzymatic hgdrolysis of polydepsipeptides with functionalized pendant groups. Macromol Chem Phys, 1996, 197: 1823–1833
20 Ouchi T, Nozaki T, Ishikawa A, et al. Synthesis and enzymatic hdrolysis of latice acid-depsipeptide copolymers with functionalized pendant groups. J Polym Sci Part A: Polym Chem, 1997, 35: 377–383
21 Deng X M, Yao J R, Yuan M L, et al. Synthesis of poly[(glycolic acid)-*alt*-(L-glutamic acid)] and poly{(lactic acid)-*co*-[(glycolic acid)-*alt*-(L-glutamic acid)]}. Macromol Chem Phys, 2000, 201: 2371–2376
22 Guan H L, Xie Z G, Zhang P B, et al. Synthesis and characterization of biodegradable amphiphilic triblock copolymers containing L-Glutamic Acid Units. Biomacromolecules, 2005, 6: 1954–1960
23 Xie Z G, Guan H L, Chen X S, et al. A novel polymer-paclitaxel conjugate based on amphiphilic triblock copolymer. J Control Release, 2007, 117: 210–216
24 Lu C H, Chen X S, Xie Z G, et al. Biodegradable amphiphilic triblock copolymer bearing pendant glucose residues: Preparation and specific interaction with concanavalin a molecules. Biomacromolecules, 2006, 7: 1806–1810
25 Shuai X T, Ai H, Nasongkla N, et al. Micellar carriers based on block copolymers of poly(q-caprolactone) and poly(ethylene glycol) for doxorubicin delivery. J Control Release, 2004, 98: 415–426
26 Missirlis D, Kawamura R, Tirelli N, et al. Doxorubicin encapsulation and diffusional release from stable, polymeric, hydrogel nanoparticles. Eur J Pharm Sci, 2006, 29: 120–129
27 Hu Y, Xie J W, Tong Y W, et al. Effects of PEG conformation and particle size on the cellular uptake efficiency of nanoparticles with the HepG2 cells. J Control Release, 2007, 118: 7–17
28 Laurienzo P, Malinconico M, Motta A, et al. Synthesis and characterization of a novel alginate-poly (ethylene glycol) graft copolymer. Carbohyd Polym, 2005, 62: 274–282
29 Trimaille T, Mondon K, Gurny R, et al. Novel polymeric micelles for

hydrophobic drug delivery based on biodegradable poly(hexyl-substituted lactides). Int J Pharm, 2006, 319: 147–154
30 Pego A P, Poot A A, Grijpma D W, et al. Physical properties of high molecular weight 1,3-trimethylene carbonate and D,L-lactide copolymers. J Mater Sci: Mater Med, 2003, 14: 767–773
31 Zhang J X, Qiu L Y, Jin Y, et al. Controlled nanoparticles formation by self-assembly of novel amphiphilic polyphosphazenes with poly (N-isopropylacrylamide) and ethyl glycinate as side groups. React Funct Polym, 2006, 66: 1630–1640
32 Chu B, Zhou Z. Physical chemistry of polyoxyalkylenene block copolymers. Surf Sci Ser, 1996, 60: 67–144
33 Giacomelli C, Borsali R. Morphology of poly(ethylene oxide)-block-polycaprolatone block copolymer micelles controlled via the preparation method. Macromol Symp, 2006, 245/246: 147–153
34 Jain S, Bates F S. Consequences of nonergodicity in aqueous binary PEO-PB micellar dispersions. Macromolecules, 2004, 37: 1511–1523
35 Zhang L, Eisenberg A. Multiple morphologies and characteristics of "crew-cut" micelle-like aggregates of polystyrene-*b*-poly(acrylicacid) diblock copolymers in aqueous solutions. J Am Chem Soc, 1996, 118: 3168–3181
36 Ouchi T, Miyazaki H, Arimura H, et al. Formation of polymeric micelles with amino surfaces from amphiphilic AB-type diblock copolymers composed of poly(glycolic acid lysine) segments and polylactide segments. J Poly Sci: Part A: Poly Chem, 2002, 40: 1426–1432
37 He Y Y, Zhang Y, Xiao Y, et al. Dual-response nanocarrier based on graft copolymers with hydrazone bond linkages for improved drug delivery. Colloid Surface B, 2010, 80: 145–154
38 He Y Y, Zhang Y, Gu C H, et al. Micellar carrier based on methoxy poly(ethylene glycol)-block-poly(ε-caprolactone) block copolymers bearing ketone groups on the polyester block for doxorubicin delivery J. Mater Sci: Mater Med, 2010, 21: 567–574
39 Akimoto J, Nakayama M, Sakai K, et al. Molecular design of outermost surface functionalized thermoresponsive polymeric micelles with biodegradable cores. J Poly Sci: Part A: Poly Chem, 2008, 46: 7127–7137
40 Hoes C J T, Boon P J, Kaspersen F, et al. Design of soluble conjugates of biodegradable polymeric carriers as adriamycin. Makromol Chem Macromol Symp, 1993, 70/71: 119–136
41 Patri A K, Majoros I J, Baker J R. Dendritic polymer macromolecular carriers for drug delivery. Curr Opin Chem Biol, 2002, 6: 466–471
42 Kataoka K, Harada A, Nagasaki Y. Block copolymer micelles for drug delivery: design, characterization and biological significance. Adv Drug Deliv Rev, 2001, 47: 113–131
43 Yoo H S, Lee K H, Oh J E, et al. *In vitro* and *in vivo* anti-tumor activities of nanoparticles based on doxorubicin-PLGA conjugates. J Control Release, 2000, 68: 419–431
44 Sun Y, Yan X L, Yuan T M, et al. Disassemblable micelles based on reduction-degradable amphiphilic graft copolymers for intracellular delivery of doxorubicin. Biomaterials, 2010, 31: 7124–7131
45 Savic R, Luo L B, Eisenberg A, et al. Micellar nanocontainers distribute to defined cytoplasmic organelles. Science, 2003, 300: 615–618
46 Yokoyama M, Okano T, Sakurai Y, et al. Toxicity and antitumor activity against solid tumors of micelle-forming polymeric anticancer drug and its extremely long circulation in blood. Cancer Res, 1991, 51: 3229–3236